Structural properties of cation exchange membranes: characterization,electrolyte effect and solute transfer

Alessio Fuoco, Harmen Zwijnenberg, Sylvain Galier, Hélène Roux De-Balmann, Giorgio de Luca

Structural properties of cation exchange membranes: Characterization, electrolyte effect and solute transfer

Alessio Fuoco [a,b,c,d,*], Harmen Zwijnenberg [d], Sylvain Galier [a], Hélène Roux-de Balmann [a], Giorgio De Luca [b]

[a] Laboratoire de Génie Chimique, Université de Toulouse, CNRS, INPT, UPS, Toulouse, France
[b] Research Institute on Membrane Technology (ITM-CNR), University of Calabria, Via P. Bucci, 17/C, 87036 Arcavacata di Rende (CS), Italy
[c] Department of Environmental Engineering and Land and Chemical Engineering, University of Calabria, Via P. Bucci, Cubo 44A, 87036 Rende (CS), Italy
[d] Membrane Science & Technology, University of Twente, MESA+Institute for Nanotechnology, P.O. Box 217, 7500 AE Enschede, The Netherlands

Keywords:
Ab initio modeling
Cation exchange membrane
Counter-ion effect
Transfer properties
Structural properties

A B S T R A C T

Experimental investigations have shown that the presence of electrolytes has a strong influence on the transfer of neutral organic solutes through ion exchange membranes used in electrodialysis. It was further demonstrated that this influence is due to the impact of the membrane counter-ions on the noncovalent interactions existing between the hydrated and charged polymer chains in the membrane.

The aim of this work is to investigate the structural properties of hydrated CMX membranes equilibrated with different counter-ions. Different methods, such as Infrared spectra (IR), contact angle and Differential Scanning Calorimetry (DSC) measurements, were used to characterize the membrane samples soaked in different electrolytes. In addition, IR spectra were calculated using a quantum mechanics approach and compared with the experimental ones. Shifts of characteristic IR peaks as function of membrane ionic form were observed in both experimental and computed spectra. Both spectra present shifts to lower wavenumber in presence of cations with higher hydration number. The contact angle of CMX membranes also increases in presence of more hydrated ions revealing a decrease of the hydrophilicity of the membrane. Concerning DSC, the freezing temperature of the water entrapped in the membrane polymeric network soaked with different electrolytes was measured. A shift at lower temperature was found for more hydrated trapped ions. The computational and experimental membrane structural properties were correlated with the corresponding transfer properties (sugar fluxes) and a good agreement was obtained.

1. Introduction

The increasing demand of natural resources as raw materials is difficult to face, especially in the view of sustainable development. However, nowadays, considering the balance between Earth capabilities and human demand, it is not more possible to postpone the introduction of sustainable development constrains [1]. A possible way to contrast the increasing human demand is the process intensification that means improvement in plant efficiency, minimization of energy consumption and waste production, thus reducing costs and environmental impact.

Membrane technologies can play a primary role considering their lower energy consumption (in comparison with traditional methods), their capability to transport in an efficient and selective way specific compounds (recycling of water, chemicals and/or raw material), while their potential to boost the reaction processes and scale up can decrease the plants size [2–4].

In the frame of process intensification for complex fluids, the electrodialysis has found a second life. In the past decades, electrodialysis was widely applied in brackish water desalination, but nowadays, its potentialities are investigated to improve the process performances in chemical, food and pharmaceutical industries such as: wine productions (cold stabilization), deacidifications of fruit juice, whey demineralization, treatment of brines or lixiviates, production of green chemicals building blocks (organic acids), purification of saccharides, textile industry waste treatment [5–9].

However, the bottleneck for the spreading of membrane applications is in their high sensitivity to the composition of the feed solution, which makes the prediction of system performance difficult. A strong impact of the ions on the membrane transport properties was discovered in nanofiltration (NF) and electrodialysis (ED) processes. Most of the results, found in literature,

* Correspondence to: Institute on Membrane Technology, ITM-CNR, Via P. Bucci, c/o University of Calabria, Cubo 17/C, 87030 Rende (CS), Italy.
E-mail addresses: a.fuoco@itm.cnr.it, a.fuoco@europe.com (A. Fuoco).

http://dx.doi.org/10.1016/j.memsci.2016.07.031

concern the case of NF and only few of them the case of ion exchange membranes used in ED. For instance, the influence of the ionic composition on the transfer of a neutral solute through nanofiltration membranes was first reported by Wang et al. [10] in the case of sugar (glucose or sucrose)/NaCl solutions. It was shown that the transfer of sucrose is weakly affected by the presence of the electrolyte. On the contrary, the transfer of glucose was found to increase for increasing NaCl concentrations. In 2005, Bouchoux et al. [11] have established a relationship between the hydration of the ions and the mass transfer increase of glucose in presence of salt. Boy et al. [12] made a step forward, pointing out that the diffusion flux of sugars (xylose, glucose and sucrose) through a NF membrane, in presence of various electrolytes (NaCl, Na_2SO_4, $CaCl_2$, $MgCl_2$), is mainly fixed according to the influence of the electrolyte on the solute properties. Other evidences of the salts effect on the transfer of organic molecules through NF membranes have been also observed with PEG (poly ethylene glycol). The transfer of this molecule was investigated by Bouranene et al. [13] for inorganic NF membrane, as well as by Escoda et al. [14] with an organic NF membrane. Both works have demonstrated that the presence of salts (KCl, LiCl, $MgCl_2$) increases the transfer of PEG trough the membrane and that the salt effect depends on its concentration as well as on its hydration. Electrodialysis can be applied in the separation of small organic ions from salts [15,16], but only few work are focused on the electrolyte effect on the transport properties of the membrane. In particular, in a recent work dealing with the transfer of neutral organic solutes through cation-exchange membrane in diffusion condition, Galier and Coworkers [17] found that the fluxes of three sugars, through a CMX membrane (Neosepta) equilibrated with Na^+ are more than twice with respect to the fluxes through the same membrane but equilibrated with Mg^{2+}. Moreover, using a specific procedure, able to discern whether the effect of ions is caused by their presence in the solution or in the membrane (as counter-ions), they pointed out that the ions inside the polymer matrix are the principal cause for the observed trend. A successive quantum and molecular mechanics modeling work showed that the noncovalent interaction energy per water molecule or water wire between hydrated polymer chains and equilibrated with different cations correlates with the sugar fluxes values and depends on the counter-ion. A water wire is defined as the shortest path of water molecules connecting two oxygen atoms of SO_3^-groups located in two different chain fragments of the membrane [18].

The analysis of the effects of various electrolytes on some key characteristics of CMX membrane is the aim of this work. To achieve this objective, experimental characterizations and calculation of infrared peaks are carried out. Hence, this work provides useful information to understand, at the molecular level, the mechanisms at the basis of the performance of these membranes in similar conditions. Moreover, this work aim to be a nice starting point for future fundamental works concerned with the mechanisms of organic and inorganic solute transfer through membranes for electrodialysis, taking into account the effect of applied current density and other process parameters.

The infrared spectra of a CMX membrane soaked in various electrolytes, are calculated in the framework of Density Functional Theory and compared with measured experimental spectra. In fact, molecular vibrations are very sensitive to changes in the environmental conditions. A relationship between the presence of different cations and the shift of characteristic infrared peaks was demonstrated by Falk [19] with Nafion based membranes. In particular, he has pointed out that, in Nafion membrane, the effect of the cation is highly identifiable in the water and SO_3^- vibrational modes properties, influencing the energy of these vibrations, thus their position in the IR spectra.

Both contact angle and differential scanning calorimetry (DSC) methods are also used in this work. The first was chosen for its simplicity and because it is known that changes in contact angle are related to modifications in the membrane surface properties. Thus, this is a way to characterize the feed-membrane interface according to the environmental conditions. DSC is also used as it gives information on the sample bulk allowing investigation of the state of the water molecules in the membrane as function of the different cations [20,21].

2. Materials and methods

2.1. Infrared frequencies computational details

The IR spectra were computed in the framework of the Density Functional Theory (DFT) by using the hybrid functional X3LYP [22]. Structural models, formed by one cation, one or two functionalized monomers and one water molecule, were used to describe the noncovalent interactions between the cation functional groups and water molecule. In order to take into account different water arrangements in the models containing divalent cations, two initial configurations were considered for Mg^{2+} and Ca^{2+} cations: the first, with one water molecule in a central position with respect to the two SO_3^- groups and the other more external. More information on the construction of the molecular models used in the computational IR analysis can be found elsewhere [23]. The model geometries were fully optimized to a minimum of energy after which the vibrational analysis was performed.

Since the aim of this work is a qualitative comparison between theoretical and experimental vibrational frequencies in order to elucidate the counter-ions effect, these simple models can be considered appropriate for this purpose. A starting geometry with the same high theory level was not available for NH_4^+, thus the vibrational modes of this cation were not computed here.

All the calculations were performed by NWChem 6.1 [24], an ab initio computational chemistry software package with extensive capabilities for large scale simulations of chemical systems. Triple-ζ basis sets were used for the geometry optimization and the vibrational analysis. On C, H, S and O atoms a "6–311G*" basis set was applied while the "6–311+G*" set was used on the cations. The reliability of the used basis sets and functional was tested in previous works [25,26]. The convergence criteria for the optimization of the model geometries, based on Cartesian displacement and gradient thresholds were set as tight [27], while the energy convergence threshold, for the self-consistent field procedure, was imposed to 10^{-8} a.u. and the root-mean-square of the electron density to 10^{-6} a.u.

2.2. Membrane and membrane conditioning

The membranes used in this work are CMX membranes (Neosepta), cation exchange membranes of sulfonated polystyrene-divinylbenzene. Before the characterizations, the membrane samples were conditioned following the NF X 45-2000 standard procedure [17]. This treatment consists of a washing cycle with acid (HCl), base (NaOH) and electrolyte solutions to clean the membrane from eventual impurities due to the manufacturing process and to equilibrate the membrane with the different cations. The complete procedure is reported in previous work [17,23]. The differently equilibrated membranes were stored in their own electrolyte solutions. Before performing the analysis such as IR and DSC, the membrane was washed in ultrapure water to remove the excess of salt. The ultrapure water in the washing bath was exchanged until no more increase of its conductivity was measured. For all the electrolyte solutions, only salts containing chloride as anion were used in order to avoid any secondary effects that could

be due to different anions: LiCl, KCl, NH_4Cl, NaCl, $CaCl_2$ and $MgCl_2$ (hexahydrate). All the chemicals were provided by Sigma Aldrich with a purity $\geq 99\%$.

2.3. Infrared spectroscopy

The IR spectra were recorded by a Nexus Diamant spectroscope equipped by an ATR accessory. The spectra were obtained by averaging 20 acquisitions over a range of wavenumber from 600 cm^{-1} to 4000 cm^{-1} with a resolution of 4 cm^{-1}. Since the broad absorption of the water in the bulk and on the surface could overlay the whole range of the spectra, the samples were dried in oven at 50 °C for 48 h before the data acquisition. This low temperature was chosen to exclude any possible influence of a thermal stress on the samples. The data elaboration was performed using OMNIC software.

2.4. Contact angle

Contact angles of CMX membranes soaked in different electrolyte solutions were studied using the captive bubble technique [28,29]. The thermodynamics of contact angles between a liquid and a solid is well described by Young's equation [30] and the output of his work was crucial for the development of Good and Girifalco [31,32] equation by which the surface free energy of the membranes can estimated:

$$\gamma_s = \frac{\gamma_l(1+\cos\theta)^2}{4\Phi^2}$$

where γ_s is the surface free energy of the membrane, γ_l is the surface free energy of the liquid, θ is the equilibrium contact angle and Φ is an interaction parameter related to intermolecular forces (polar, dispersive, etc.). In this work, Φ can be approximated as 1 due to the close matching between the molecular properties and the intermolecular forces of both phases [31], i.e. the membrane can form strong hydrogen bonds with water [33]. The values of γ_l for the different aqueous solutions is calculated by the Dutcher-Wexler-Clegg method [34]. Thus, it is possible to estimate the surface free energy of the CMX membranes soaked in LiCl, KCl, NH_4Cl, NaCl, $CaCl_2$ and $MgCl_2$ solutions by measurements of their contact angle in the different environments.

The contact angle measurements were performed at room temperature pumping 6 µl of air to the underside of the membrane and releasing the bubble by the computer controlled micro syringe of the Dataphysics contact angle system OCA 20. The measurements were repeated at least five times in different spots resulting in 10 data points since two angles (left and right sides) can be measured.

2.5. Differential scanning calorimetry

The cooling and heating cycles of the CMX membrane conditioned following the NF X 45-2000 standard procedure [17] in KCl, NaCl, LiCl, NH_4Cl, $CaCl_2$ and $MgCl_2$ were measured on a Perkin Elmer DSC 8000. The surface of each membrane was first lightly wiped to remove superficial water. Thus, samples with a weight in the range of 8–12 mg were sealed in an aluminum pan and equilibrated for 1 min at 30 °C. Subsequently, each sample was cooled at −60 °C with a scanning rate of 5 °C/min, stabilized for 3 min at this temperature and then heated to 30 °C with the same scanning rate. The cycle was repeated three time for each sample. The reiteration of the cycles was necessary because in the first cycle, the position of the peak at the freezing temperature was not found in a stable position. This incertitude can be attributed to different responses of the polymer network to the water volume expansion due to the transition phase. However, after the first cycle, the peaks are reproducible. This means that, after the first mechanical stress (enlargement of the chain-chain distances due to the water expansion), the membrane has a well-defined characteristic.

3. Results and discussion

3.1. Theoretical and experimental vibrational frequencies (Infrared spectra)

The accurately optimized geometries of the chemical model, i.e. the cation-monomers adducts/complexes are reported in the Supporting information (Figs S.1–S.5). These structures were analyzed for the further assignment of the absorption IR bands and their structural properties are discussed together with the IR computed spectra.

The calculated IR spectra, relative to these models, are reported in Figs. 1–5, while the more significant bond lengths of these optimized structures are reported Tables S.1–Table S.3 of the Supporting information. The complete lists of assignments for each computed vibrational mode, and a deeper discussion about the structural properties are reported elsewhere [23].

The quantum calculations give a shift of the characteristic O–H stretching, forming hydrogen bonding with the oxygen of the SO_3^- group, at 3461 cm^{-1} for Na^+ (Fig. 1), and at lower values in the case of Mg^{2+} (Figs. 4 and 5), i.e. 3234 cm^{-1} and 3217 cm^{-1} associated to the structures of Figs. S.4 and S.5 respectively. The optimized structure containing Ca^{2+} and the water in external position (Fig. S.3) shows an O–H shift similar to the stretching associated to the Mg^{2+} structures. Instead, the optimized structure having the water in central position shows two vibrational modes for the O–H stretching in interaction with the sulfonic groups: symmetrical and asymmetrical stretching (3469 cm^{-1} and 3530 cm^{-1}). The computed wavenumber of symmetrical vibrational mode is similar to the O–H stretching of the water in the structure with Na^+, while the asymmetrical mode is obtained at a slightly higher wavenumber.

It is worth noting that the stretching of the O–H groups that do not form hydrogen bonds with the oxygen of SO_3^- are very similar in all the structures containing Na^+, Mg^{2+} and Ca^{2+} with the water molecule in the external position, 3865 cm^{-1}, 3875 cm^{-1}, 3878 cm^{-1} and 3891 cm^{-1}, respectively. The Ca^{2+} structure with the water in a central position does not have this vibrational mode since both the O–H interact with the sulfonic groups.

Hydrogen bond between water molecule and SO_3^- group is affected by the nature of cation. In fact, with cation having higher interaction with water molecule, the peak related to the stretching of the O–H, with hydrogen atom forming a bond with the SO_3^- group, is shifted to lower wavenumber as the strength of O–H

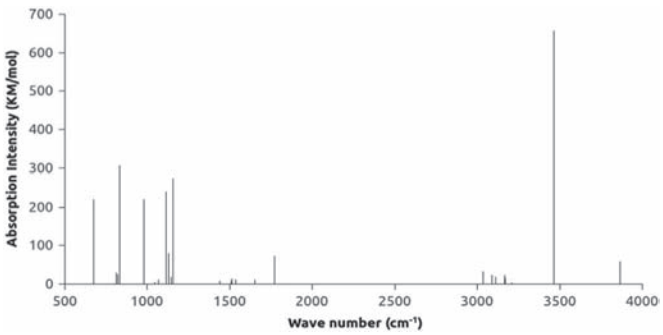

Fig. 1. QM computed IR spectra of functionalized styrene-Na^+…H_2O adduct (Fig. S.1).

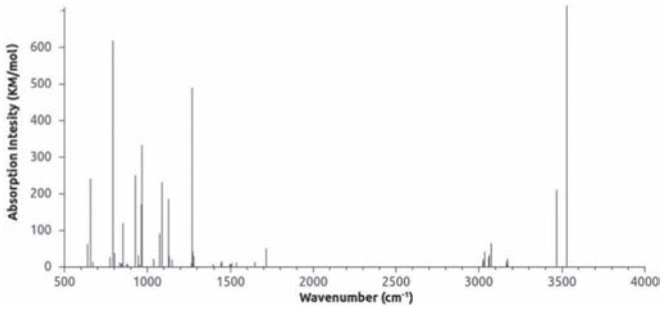

Fig. 2. QM computed IR spectra of functionalized styrene-Ca^{2+}…H_2O adduct. Initial position of H_2O: internal (Fig. S.2).

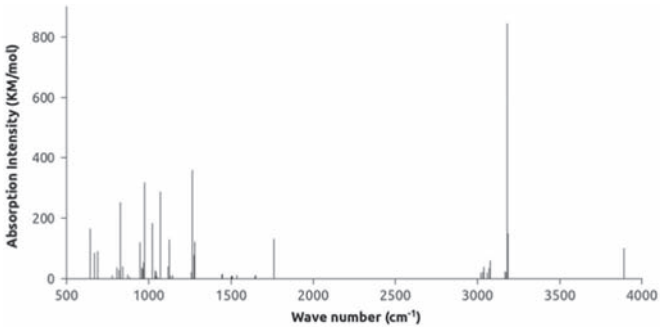

Fig. 3. QM computed IR spectra of functionalized styrene-Ca^{2+}…H_2O adduct. Initial position of H_2O: external (Fig. S.3).

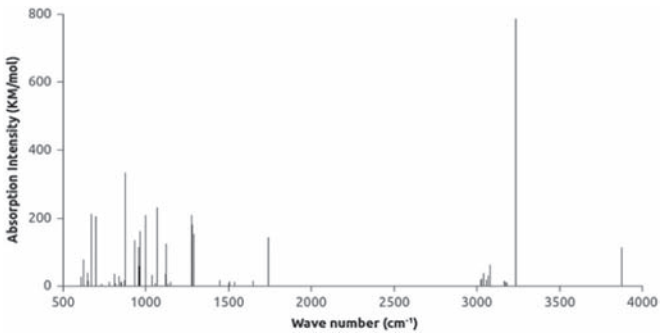

Fig. 4. QM computed IR spectra of functionalized styrene-Mg^{2+}…H_2O adduct. Initial position of H_2O: internal (Fig. S.4).

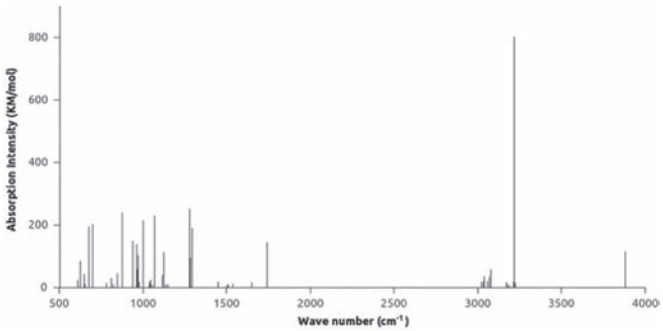

Fig. 5. QM computed IR spectra of functionalized styrene-Mg^{2+}…H_2O adduct. Initial position of H_2O: external (Fig. S.5).

bond decreases due to its double interaction with the cation and functional group. Cations showing higher interaction energy with water and functional group ($Mg^{2+} > Ca^{2+} > Na^{+}$) affect the structure of these adducts leading to a rearrangement of the electron density of water molecule. This interpretation is confirmed by the changes in the cation-functional group distance, evaluated as the distance between the cation and the nearest oxygen of the functional group. These distances are 2.3 Å for Na^{+}, 2.1 Å for Ca^{2+} and 1.9 Å for Mg^{2+}. These computed distances are slightly smaller than the ones computed previously [18], however this small difference of 0.1 Å is in a normal error range of computational models and it is due to the differences in the two molecular models, as well as the differences in the two used level of theory. It is important to note that a smaller distance means a stronger interaction between the functional group and the counter-ion. This attractive interaction modifies the electron density of the near environment, and affect, like a domino effect, the non-covalent interactions among the coordinating water molecules involved in the chain-chain cohesion energy as illustrated in a previous work [18].

In addition to the O–H stretching, the scissoring vibrational modes of the water molecules, show a cation dependence. As in the previous case, a shift to lower wavenumbers is observed with values of 1772 cm^{-1}, 1761 cm^{-1} and 1741 cm^{-1} for similar structures containing Na^{+}, Ca^{2+} (Fig. S.3) and Mg^{2+}, respectively, i.e. with the optimized water molecules in the external position. For the adduct with the Ca^{2+} in central position, an associated wavenumber of 1716 cm^{-1} is found for the water scissoring vibrational mode.

Together with the scissoring mode, also the structural properties of the water molecule are affected by the nature of the cation. The optimized O–H bond lengths and angles of the water molecules coordinating the cations in the models used in the vibrational analysis are reported at the bottom of Tables S.1–S.3 for Na^{+}, Ca^{2+} and Mg^{2+} respectively. Moreover, a single water molecule was optimized in *vacuum* at the same level of theory for comparison. O–H bond lengths of 0.962 Å and angle of 105.9° were obtained.

The stronger variation with respect to the value of the bond angle in *vacuum* was observed in the structure containing the Ca^{2+} with the water in a central position (Fig. S.2). In this case, the angle increases of about 5°, while variations of 3° and 4° were found for the other structures containing Ca^{2+} and Mg^{2+}, respectively. Otherwise, Na^{+} has a very small influence on the H–O–H angle.

The bond lengths analysis (O7-H1 and O7-H2 for Na^{+}, Ca^{2+} and Mg^{2+}) reveals a loss of symmetry (present in the water in vacuum), due to the stretching of the O–H bonds for the hydrogen bonding between the O–H and one oxygen of the functional group. The change in the O–H length (i.e. 0.961 Å and 0.996 Å in the complex with Mg^{2+}) discloses that the attractive interaction between the hydrogen of water and the functional group is strong since the O–H bond in the water molecule is stretched in the direction of the functional group.

The characteristic absorption peaks of the S–O vibrational modes are shifted to lower wavenumbers following the interaction energy trend: $Na^{+} < Ca^{2+} < Mg^{2+}$. This cation-dependent shift reflects a weakening of the S–O bond strength due to a modification in its electron density. The cation showing higher interaction with the sulphonyl's oxygen attracts its electrons producing the computed and observed S–O stretching shift as function of cation nature. This interpretation is also confirmed by the variation of the S–O length as will be discussed later.

The absorptions at 1155 cm^{-1} in the Na^{+} spectrum, 1069 cm^{-1}, 1075 cm^{-1} and 1087 cm^{-1} (associated to the two models containing Ca^{2+}) and the 1067 cm^{-1}, associated to the Mg^{2+} structures, can be assigned to the S–O stretching. The greatest S–O shifts to lower energy in systems containing Ca^{2+} and especially Mg^{2+} reveal a strong interaction of these cations with the functional groups. A similar trend is also observed for the asymmetrical and symmetrical ensemble stretching of the $–SO_3^{-}$

group as shown in Figs. 2–5 starting from 1115 cm^{-1} for the optimized structures with Na^{+} down to a lower wavenumber of 979 cm^{-1} for Ca^{2+} and Mg^{2+}. The presence in the computed spectra of multiple frequencies, (e.g. 996 cm^{-1} and 934 cm^{-1} in the case of Mg^{2+}; Fig. 5), related to the symmetrical stretching proves that the cation-functional group distance plays an important role on the interactions; Indeed it shows that the farer functional groups are also influenced and the longer is the distance, the weaker is the influence. The presence of a cation-dependent shift in all computed $–SO_3^-$ vibrational modes is a strong evidence of the cation influence. On one hand, the different vibrational modes are proofs of the counter-ion capability to interact with the polymer matrix changing the physical and transport properties of the membrane itself. On the other hand, the cation dependent shift is also a proof of the interaction between the counter-ion and the water molecules entrapped in the polymer matrix.

The bond lengths analysis shows interesting correlation between the cations-SO_3^- distance and the properties of the functional group itself. In each structure, the S–O bond, closer to the cation, is longer than the other ones; specifically, the lengths of these S–O bonds decrease when the distance between the inquired S–O and the cation increases. The length of the S–O bonds closer to the cation depends also on the nature of the ion. Indeed the S–O distances are longer for Mg^{2+} (1.540 Å) with respect to Ca^{2+} (1.531 Å) and Na^{+} (1.499 Å). The changes of the S–O length as function of the cation nature can be correlated to the attraction between the partial negative charges on the $–SO_3^-$ and the positively charged ions reducing the nearest oxygen-cation distance, i.e. the S–O distance is stretched to allow the oxygen-cation approach.

To validate the conclusions/findings obtained from quantum mechanics calculations, the experimental infrared spectra of the CMX membrane, soaked in Na^{+}, Ca^{2+}, Mg^{2+} are reported in the Figs. 6–9 and discussed below. In addition to the IR spectra of the membranes equilibrated with monovalent ions, the spectrum of a membrane soaked with the ammonium ion was also measured and reported in Fig. 9.

In the experimental spectra, the presence of wide absorption over 3000 cm^{-1} reveals a non-negligible presence of water molecules even if the samples were prior dried for 48 h at 50 °C. In fact, a broad absorption zone is detected, and it can be associated to the stretching of the O–H bonds in the water molecules in interaction with other water molecules. However, the sharpest and highest peaks present in this region can be associated to the O–H bonds in interaction with the functional group of the membrane.

The influence of the different chemical environments, i.e. the presence of a different counter-ion in the system, produces a shift in these resulting peaks, as shown in Fig. 6–8. In fact, the experimental peaks of the O–H stretching obtained with Na^{+}, Ca^{2+} and Mg^{2+} are found at 3446 cm^{-1}, 3414 cm^{-1} and 3387 cm^{-1}, respectively. This is in agreement with the above computed results

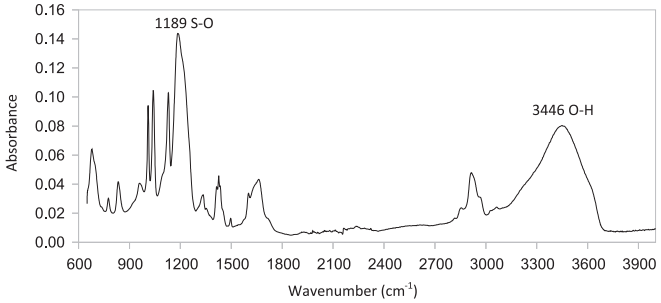

Fig. 6. Experimental IR spectra of CMX membrane equilibrated by Na^{+} as counter-ion.

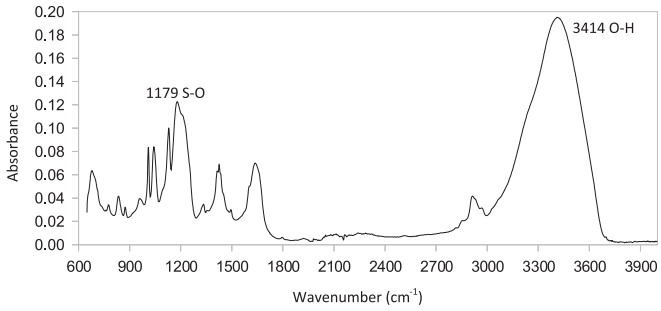

Fig. 7. Experimental IR spectra of CMX membrane equilibrated by Ca^{2+} as counter-ion.

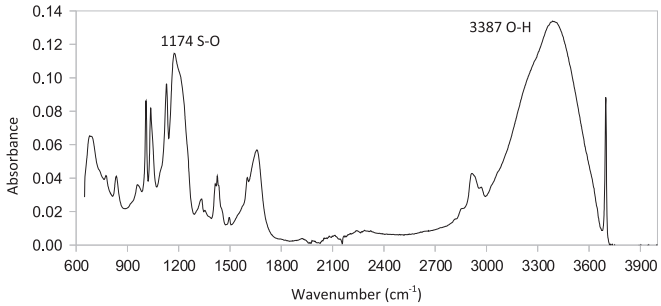

Fig. 8. Experimental IR spectra of CMX membrane equilibrated by Mg^{2+} as counter-ion.

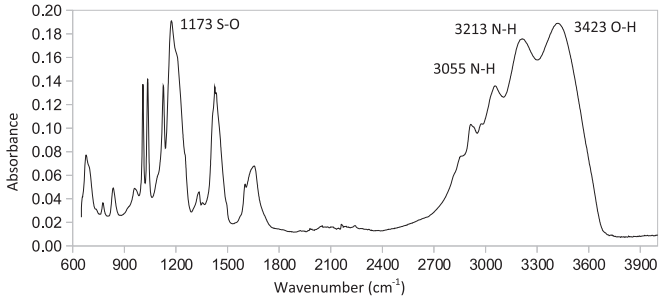

Fig. 9. Experimental IR spectra of CMX membrane equilibrated by NH_4^{+} as counter-ion.

showing the same trend for the O–H shift as function to the counter-ion nature. The shift to lower wavenumbers for the Ca^{2+} and Mg^{2+} complexes shows that the stretching modes of the O–H, forming hydrogen bonding, are energetically weaker with more hydrated counter-ions in solution [35]. This result is physically consistent since weaker O–H bonds means that the hydrogen forms stronger H-bonds with the SO_3^-…Mg^{2+} or Ca^{2+} adducts than with Na^{+}. This finding allows establishing a relationship between the counter-ion equilibrating the membrane and its transport properties. As shown in the previous work, stronger H-bonds between water and $–SO_3^-$ functional group, coordinating the different counter-ions, imply lower sugar fluxes through the membrane. Thus, the shift of O–H frequencies as function of the tested cations, experimentally and theoretically found, is a further evidence to confirm the proposed mechanism to explain the influence of these cations on the sugar transport [18].

In the experimental spectrum of the membrane equilibrated with Ca^{2+} (Fig. 7), the presence of water in several configurations does not allow the separation of the symmetrical or asymmetrical O–H stretching as noted above.

Unfortunately, due to experimental limitations (instrument resolution) the experimental peaks related to the scissoring modes of the water molecules cannot be discussed. Then no comparison

between computational and experimental data of this particular vibrational mode is feasible.

A shift based on the nature of the counter-ion is also detected in the experimental spectra in the characteristic zone of symmetric S–O stretching, close to 1180 cm^{-1}. More precisely, intense absorption bands are detected at 1186 cm^{-1} for Na^+, 1179 cm^{-1} for Ca^{2+} and 1174 cm^{-1} for Mg^{2+}. Even if the difference between the wavenumbers related to this vibration for the system with Na^+ and Ca^{2+} is close to the resolution of the instrument, the effect of divalent cations is visible in a shift of the S–O stretching band to lower wavenumbers with respect to monovalent cations.

A particular case is the IR spectra of the CMX membrane equilibrated by NH_4^+ (shown in Fig. 9). Indeed, the vibrational behavior of the N–H bond is similar to the characteristic water O–H vibrational modes. From the corresponding experimental spectrum, in the called "water zone" (over 3000 cm^{-1}), a broad absorption is present in which three peaks are predominant at 3423 cm^{-1}, 3213 cm^{-1} and 3055 cm^{-1}. The last peaks correspond to asymmetrical and symmetrical stretching of the ammonium N–H bonds, while the first one is due to the overlap of the stretching modes of water molecules. Considering the aforementioned relationship between O–H stretching modes and the sugar fluxes ($J_{NH4^+} > J_{Na^+} > J_{Ca2^+} > J_{Mg2^+}$) [17], the above peak related to the stretching modes of water falls at an unexpected wavenumber since it was supposed to be found at higher wavenumber for membrane equilibrated with NH_4^+. In fact, considering the trend of the O–H wavenumbers for membranes with monoatomic ions ($Na^+ > Ca^{2+} > Mg^{2+}$), the peak of the H_2O vibrational modes, experimentally observed at 3423 cm^{-1} with the membrane equilibrated with NH_4^+, was expected to be obtained at higher wavenumber than the peak for the same vibration obtained with Na^+ as counter-ion (3446 cm^{-1}). The same unexpected behavior was observed for the membrane equilibrated with NH_4^+ for the absorption peak related to the S–O stretching. Indeed it is found at 1173 cm^{-1} while it was expected at values at least slightly higher than 1186 cm^{-1}.

A possible explanation for these unexpected shifts can be because the NH_4^+ is not a monoatomic cation unlike other ones considered in that work. At the same time, the N–H bond favors the formation of H-bonds with the sulfonated group and/or the water molecules that can affect its vibrational mode. In fact, the formation of one H-bond with the water molecule and/or with the SO_3^- group can give an "anchor"/shield" effect that decreases the absorption wavenumber. These strong interactions can be emphasized in the preparation of the sample, in particular during the drying step. In fact, with the extraction of the water molecules from the polymer matrix, the ammonium-SO_3^- interactions are favored since water molecules that could act as a shield are removed. Furthermore, a sort of weak acid-base interaction could play a role in the band shifts i.e. a partial protonation of the functional groups.

Even with some limitations, these data show that IR spectroscopy is a powerful technique to investigate ion-membrane interactions, particularly when interaction spots like the functional groups are present in the polymeric network. The shift at lower wavenumbers can be related to stronger functional groups-water hydrogen bonds, showing that the long and short noncovalent interactions per water molecule or wire between the polymeric chains depend on the nature of the cation.

3.2. Contact angle measurements

Table 1 gives the values of the contact angles obtained for the CMX membrane equilibrated with different cations. It should be remembered that a surface is "mostly hydrophilic" when $\theta < 90°$, and "mostly hydrophobic" when $\theta > 90°$. Since for all the conditions θ is lesser than 90° one can conclude that the CMX membrane is mostly hydrophilic. Moreover, contact angle measurements point out a remarkable influence of the counter-ion on the hydrophilic character of the membrane as shown from the different values of θ as function of the solution in which the membrane is soaked. The smaller contact angle is observed for the membrane soaked in NH_4Cl, while the higher is observed for the membrane equilibrated by $MgCl_2$. One can deduce that for increasing counter-ion hydration, the CMX membrane hydrophilicity decreases as the following trend:

$$NH_4^+ > K^+ > Na^+ > Li^+ > Ca^{2+} > Mg^{2+}$$

Table 1
Measured contact angles θ, solution surface free energy γ_l, and membrane surface free energy γ_s. *Li value not available by Dutcher-Wexler-Clegg method.

Aqueous solutions (0.1 M)	$\theta \pm \sigma$ (°)	γ_l (mJ m^{-2}) [34]	γ_s (mJ m^{-2})
NH_4Cl	23.2 ± 0.3	72.12	66.40
KCl	23.6 ± 1.2	72.15	66.24
NaCl	24.9 ± 0.1	72.16	65.61
LiCl	25.9 ± 0.3	N/A*	–
$CaCl_2$	32.6 ± 1.4	72.39	61.43
$MgCl_2$	45.7 ± 0.4	72.37	52.18

The role of ions can be imputable to a modification of the sulfonated group capability to interact with the external water molecule, or rather as a sort of screening effect of the ions on the hydrophilic sulfonated groups. In fact, in Table 1 a clear influence of the counter-ion on the membrane contact angle is visible. Higher is the interaction energy of the counter-ion, bigger is the contact angle. Variations in the contact angle reveal a change of the surface free energy of the membrane. In Table 1 the surface free energy values (γ_s) of the CMX membrane soaked in different electrolytes, calculated from measured contact angles and surface free energy of the liquid (γ_l) using Dutcher-Wexler-Clegg method, are reported [34]. After the correction for the liquid properties, the trends of the impact of the electrolytes on the membrane surface also follow the hydration number trend. Fig. 10 shows the variations of the fluxes of some saccharides as measured in a previous work in diffusion regime though the same CMX membrane versus the surface free energy of the membrane soaked in different electrolytes (NH_4^+, Na^+, Ca^{2+}, Mg^{2+}). One can observe that a good correlation is obtained. More precisely, the mass transfer increases for increasing surface free energies.

The contact angle measurements can be also compared with the computational work carried out in the framework of Quantum

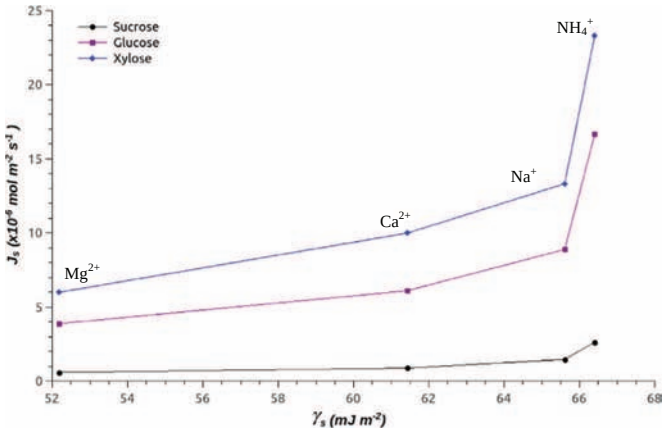

Fig. 10. Sugar fluxes vs surface energies of CMX membrane in several ionic forms (Mg^{2+}, Ca^{2+}, Na^+ and NH_4^+). Sugar fluxes measured in diffusion regime [Sugar] = 1 mol L^{-1} [electrolyte] = 1 equiv. L^{-1} [17].

Mechanics/Molecular Mechanics theory in a previous work [18]. In that prior work, the chain-chain interaction energies in the polymer network constituting the CMX membrane were computed in presence of 3 different cations (Na^+, Ca^{2+}, and Mg^{2+}). The chain-chain interactions of the membrane soaked in presence of Ca^{2+} or Mg^{2+} were found respectively 1.5 times and 2.5 times stronger than the chain-chain interactions of the membrane soaked with Na^+. Thus, a higher cohesion energy between the polymer chains corresponds to a less hydrophilic membrane, since the water molecules cannot interact with the polymeric matrix.

Moreover, considering that cations with higher hydration numbers have also higher hydration energies, one can suppose that they can induce stronger intra-system interactions. Consequently, the probability that a functional group of the polymer network interacts with an external molecule is lower. The fact that divalent cations bind to two functional groups, probably introduces the effect that a part of the functional groups is pulled away from the surface to associate with cations located inside the membrane. As such, it can be envisaged that the surface concentration of the sulfonic groups may be lower in presence of divalent cations as compared to monovalent ones. This kind of shielding effect could decrease the membrane hydrophilicity. Additionally, in the case of less hydrated counter-ion, their ability to promote intra-surface interactions is weaker, thus the probability that an SO_3^- group interacts with the environment is higher.

3.3. *Thermal properties*

Thermal properties can be used to characterize the state of water confined in the CMX membrane equilibrated by different cations, which has different properties with respect to the water in the bulk. Indeed, due to the interactions with the membrane, the water can have three different states: free water, freezable water and non-freezable water [36].

The peak at 0 °C which would correspond to the free water is not detected, that means that all the water enclosed in the membrane is affected by the polymer matrix. In Fig. 11, the characteristic peaks of the freezable water in the membrane are reported for each counter-ion investigated (NH_4^+, K^+, Na^+, Li^+, Ca^{2+} and Mg^{2+}). Supercooled freezing water peaks are detected in the temperature range between -12 and -20 °C, depending on the counter-ion used to equilibrate the CMX membrane. More precisely, decreasing supercooled freezing temperatures ($NH_4^+ > Na^+ \approx K^+ \approx Li^+ > Ca^{2+} > Mg^{2+}$) are obtained for increasing counter-ion hydrations ($NH_4^+ < K^+ < Na^+ < Li^+ < Ca^{2+} < Mg^{2+}$). It is worth noting the overlap of the freezing peaks for three similar monovalent and monoatomic cations (Na^+, K^+ and Li^+).

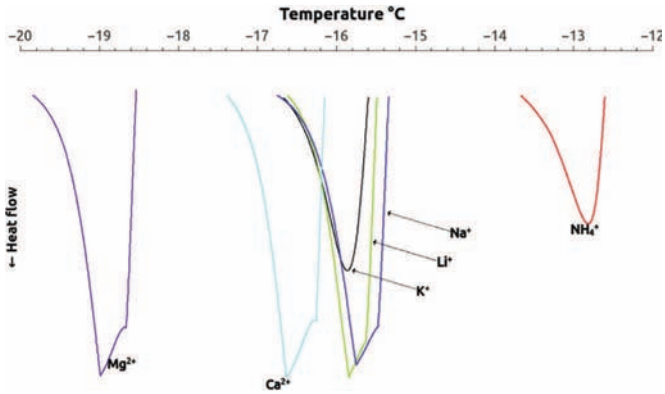

Fig. 11. DSC cooling peaks for CMX membrane equilibrated by different counter-ions.

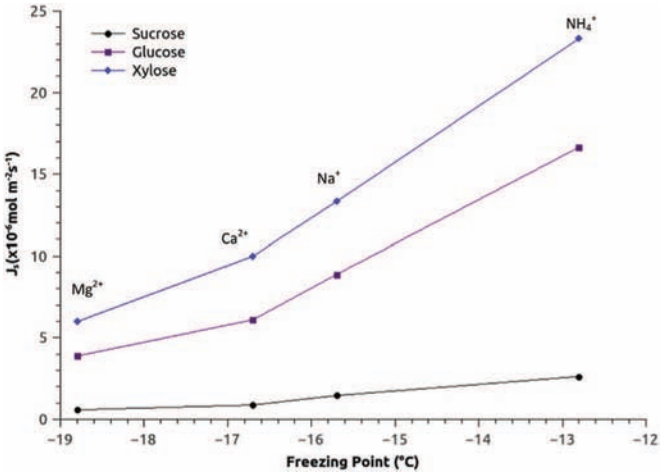

Fig. 12. Sugar fluxes in function of the freezing temperature of water entrapped in CMX membrane soaked in different electrolytes. Sugar fluxes measured in diffusion regime [Sugar] = 1 mol L^{-1} [electrolyte] = 1 equiv. L^{-1} [17].

A good correlation is obtained between the decreasing sugar fluxes through the CMX membrane and the decreasing freezing temperature as function of the counter-ion as shown in Fig. 12. More precisely, lower freezing temperatures is observed for increasing counter-ion hydration, which in its turn is correlated to lower sugar fluxes. This suggests that the freezing point of the water entrapped in the membrane is directly affected by the structural property of the membrane that influences also the transfer of sugar.

The shift to lower temperatures of the freezing point of the freezable water according to the cation reveals a change in the state of the water due to the change of cohesion energy between polymer chains in function of the cation equilibrating the membrane. Higher is the hydration of the cation equilibrating the membrane (and its interaction energy), higher is its impact on the diffusion of the solutes through the membrane. It was previously shown that the interactions between the chains are established by "interactions path" with a polymer-water-water-polymer structure. The water molecules involved in these interaction paths could give rise to the supercooling effects represented by the peaks observed at temperatures below 0 °C as shown in Fig. 11.

The temperature of the freezing peaks in the samples gives information about the differences of free volume elements size inside the membrane. In fact, the lowering of the triple point temperature of a liquid probe due to the confinement in a porous material is the basic principle of thermoporometry [37,38]. Using the Gibbs–Thomson equation [38] it is possible to affirm that the equilibrium temperature of liquid-solid phase transitions is determined by the radius of curvature at the liquid-solid interface. This radius of curvature is directly correlated to the available space. Smaller is this space, lower is the freezing temperature of the freezable liquid. In this work, the liquid phase can be always considered as water since one can assume the cations to be part of the solid phase due to their strong interactions with SO_3^- groups. Thus, the shift to lower temperature for divalent cations such as Ca^{2+} and Mg^{2+} support the hypothesis that the interstitial volume in the membrane decreases with increasing cation hydration. Unfortunately a quantitative analysis of the average free volume elements size is not possible since the developed mathematical relationships are adapted for materials with well-defined pores and in the range 2–150 nm [39,40] rather than a swollen network. Considering the decreasing sugar fluxes with decreasing freezing temperatures, it is nevertheless possible to affirm that the two physical phenomena are correlated. Furthermore, this correlation

is supported by the output of the computational modeling shown in a previous work that evidences a decreasing average distances between polymer chain fragments representative of CMX membranes equilibrated by Na^+, Ca^{2+} and Mg^{2+}.

4. Conclusion

Both the experimental and the computational spectra present a shift to lower wavenumber of characteristic peaks (O–H and S–O stretching), following the hydration scale of cations in solution. The shift to lower wavenumbers reflects an energy decrease of these vibrational modes that means a stronger interaction of the water molecules with the cation-SO_3^- complex. Moreover, energetically weaker S–O or O–H bonds in the models containing Ca^{2+} or Mg^{2+} means that the oxygen of sulfonic groups and the hydrogen of water form stronger hydrogen bonds in the Phenyl-$SO_3^-\cdots Ca^{2+}$ or Mg^{2+} adducts compared to Na^+. This shows how the divalent counter-ions bind stronger with the near water molecule than sodium ion.

Contact angle measurements have confirmed that the presence of different electrolytes changes the water affinity of the polymer matrix following the hydration of the ions in solution. The experimental data indicate that a membrane soaked with a more hydrated cation loses part of its water affinity, even if its properties remain in the range of a hydrophilic membrane. This behavior can be attributed to a decrease of the accessibility of the sulfonated functional groups due to a higher attraction with the cations.

DSC data provided the experimental proof that the state of water inside the CMX membrane changes according to the membrane counter-ion. Moving from less to more hydrated cations causes a decrease in the freezing point of the water trapped in the membrane polymer network. Since a lower freezing point of the liquid trapped in the membrane corresponds to a smaller free volume, the decreasing of the freezing point can be associated to a decrease of the volume accessible to water which is directly related to the membrane permeability to water and small neutral solutes.

The trend of the physical characterizations carried out in this work are in agreement with previous computational findings, in which the long and short noncovalent interactions per water molecule or molecular wire between the polymeric chains of the membrane follow a similar trend.

Acknowledgments

The authors would like to thank The Education, Audiovisual and Culture Executive Agency (EACEA) under the Program “Erasmus Mundus Doctorate in Membrane Engineering” – EUDIME (FPA 2011-0014, http://www.eudime.unical.it) for funding this research. In addition, they are grateful to the support of the Cineca supercomputing center.

Appendix A. Supporting information

Supplementary data associated with this article can be found in the online version at http://dx.doi.org/10.1016/j.memsci.2016.07.031.

References

[1] G.F. Network, August 19th is Earth Overshoot Day: the Date Our Ecological Footprint Exceeds Our Planet's Annual Budget, 2014.
[2] B. Van der Bruggen, E. Curcio, E. Drioli, Process intensification in the textile industry: the role of membrane technology, J. Environ. Manag. 73 (2004) 267–274, http://dx.doi.org/10.1016/j.jenvman.2004.07.007.
[3] E. Drioli, E. Curcio, Membrane engineering for process intensification: a perspective, J. Chem. Technol. Biotechnol. 227 (2007) 223–227, http://dx.doi.org/10.1002/jctb.1650.
[4] E. Drioli, A.I. Stankiewicz, F. Macedonio, Membrane engineering in process intensification—An overview, J. Membr. Sci. 380 (2011) 1–8, http://dx.doi.org/10.1016/j.memsci.2011.06.043.
[5] H. Strathmann, Electrodialysis, a mature technology with a multitude of new applications, Desalination 264 (2010) 268–288, http://dx.doi.org/10.1016/j.desal.2010.04.069.
[6] A. Elmidaoui, F. Lutin, L. Chay, M. Taky, M. Tahaikt, M.R. Alaoui Hafidi, Removal of melassigenic ions for beet sugar syrups by electrodialysis using a new anion-exchange membrane, Desalination 148 (2002) 143–148.
[7] R. Bernstein, S. Belfer, V. Freger, Toward improved boron removal in RO by membrane modification: feasibility and challenges, Environ. Sci. Technol. 45 (2011) 3613–3620.
[8] Z. Wang, Y. Luo, P. Yu, Recovery of organic acids from waste salt solutions derived from the manufacture of cyclohexanone by electrodialysis, J. Membr. Sci. 280 (2006) 134–137, http://dx.doi.org/10.1016/j.memsci.2006.01.015.
[9] C. Abels, F. Carstensen, M. Wessling, Membrane processes in biorefinery applications, J. Membr. Sci. 444 (2013) 285–317, http://dx.doi.org/10.1016/j.memsci.2013.05.030.
[10] X.-L. Wang, C. Zhang, P. Ouyang, The possibility of separating saccharides from a NaCl solution by using nanofiltration in diafiltration mode, J. Membr. Sci. 204 (2002) 271–281, http://dx.doi.org/10.1016/S0376-7388(02)00050-9.
[11] A. Bouchoux, H. Balmann, F. Lutin, Nanofiltration of glucose and sodium lactate solutions: variations of retention between single- and mixed-solute solutions, J. Membr. Sci. 258 (2005) 123–132, http://dx.doi.org/10.1016/j.memsci.2005.03.002.
[12] V. Boy, H. Roux-de Balmann, S. Galier, Relationship between volumetric properties and mass transfer through NF membrane for saccharide/electrolyte systems, J. Membr. Sci. 390–391 (2012) 254–262, http://dx.doi.org/10.1016/j.memsci.2011.11.046.
[13] S. Bouranene, A. Szymczyk, P. Fievet, A. Vidonne, Influence of inorganic electrolytes on the retention of polyethyleneglycol by a nanofiltration ceramic membrane, J. Membr. Sci. 290 (2007) 216–221, http://dx.doi.org/10.1016/j.memsci.2006.12.031.
[14] A. Escoda, P. Fievet, S. Lakard, A. Szymczyk, S. Déon, Influence of salts on the rejection of polyethyleneglycol by an NF organic membrane: pore swelling and salting-out effects, J. Membr. Sci. 347 (2010) 174–182, http://dx.doi.org/10.1016/j.memsci.2009.10.021.
[15] Y. Zhang, B. Van der Bruggen, L. Pinoy, B. Meesschaert, Separation of nutrient ions and organic compounds from salts in RO concentrates by standard and monovalent selective ion-exchange membranes used in electrodialysis, J. Membr. Sci. 332 (2009) 104–112, http://dx.doi.org/10.1016/j.memsci.2009.01.030.
[16] Y. Zhang, L. Pinoy, B. Meesschaert, B. Van der Bruggen, Separation of small organic ions from salts by ion-exchange membrane in electrodialysis, AIChE 57 (2011) 2070–2078, http://dx.doi.org/10.1002/aic.
[17] S. Galier, J. Savignac, H. Roux-de Balmann, Influence of the ionic composition on the diffusion mass transfer of saccharides through a cation-exchange membrane, Sep. Purif. Technol. 109 (2013) 1–8, http://dx.doi.org/10.1016/j.seppur.2013.02.019.
[18] A. Fuoco, S. Galier, H. Roux-de Balmann, G. De Luca, Correlation between macroscopic sugar transfer and nanoscale interactions in cation exchange membranes, J. Membr. Sci. 493 (2015) 311–320, http://dx.doi.org/10.1016/j.memsci.2015.06.028.
[19] M. Falk, An infrared study of water in perfluorosulfonate (Nafion) membranes, Can. J. Chem. 58 (1980) 1495–1501.
[20] K. Asaka, N. Fujiwara, K. Oguro, K. Onishi, S. Sewa, State of water and ionic conductivity of solid polymer electrolyte membranes in relation to polymer actuators, J. Electroanal. Chem. 505 (2001) 24–32.
[21] T. Okada, G. Xie, O. Gorseth, S. Kjelstrup, N. Nakamura, T. Arimura, Ion and water transport characteristics of Nafion membranes as electrolytes, Electrochim. Acta 43 (1998) 3741–3747.
[22] J. Cerny, P. Hobza, The X3LYP extended density functional accurately describes H-bonding but fails completely for stacking, Phys. Chem. Chem. Phys. 7 (2005) 1624–1626.
[23] A. Fuoco, Computational and experimental studies on membrane-solute interactions in desalination systems using ion-exchange membranes, Univ. Paul Sabatier (2015).
[24] M. Valiev, E.J. Bylaska, N. Govind, K. Kowalski, T.P. Straatsma, H.J.J. Van Dam, et al., NWChem: a comprehensive and scalable open-source solution for large scale molecular simulations, Comput. Phys. Commun. 181 (2010) 1477–1489, http://dx.doi.org/10.1016/j.cpc.2010.04.018.
[25] G. De Luca, F. Bisignano, a Figoli, F. Galiano, E. Furia, R. Mancuso, et al., Bromide ion exchange with a Keggin polyoxometalate on functionalized polymeric membranes: a theoretical and experimental study, J. Phys. Chem. B 118 (2014) 2396–2404, http://dx.doi.org/10.1021/jp411401v.
[26] G. De Luca, L. Donato, S. García Del Blanco, F. Tasselli, E. Drioli, On the cause of controlling affinity to small molecules of imprinted polymeric membranes prepared by noncovalent approach: a computational and experimental investigation, J. Phys. Chem. B 115 (2011) 9345–9351, http://dx.doi.org/10.1021/jp2006638.
[27] ⟨http://www.nwchem-sw.org/index.php/Geometry_Optimization⟩ visited on

11-Sept-2014, (n.d).
[28] A.W. Neumann, Contact angles and their temperature dependence: thermodynamic status, measurement, interpretation and application, Adv. Colloid Interface Sci. 4 (1974) 105–191.
[29] M.J. Rosa, M.N. de Pinho, Membrane surface characterisation by contact angle measurements using the immersed method, J. Membr. Sci. 131 (1997) 167–180, http://dx.doi.org/10.1016/S0376-7388(97)00043-4.
[30] C.J. Van Oss, M.K. Chaudhury, R. Good, Interfacial Lifshitz-van der Waals and polar interactions in macroscopic systems, Chem. Rev. 88 (1988) 927–941.
[31] R. Good, L.A. Girifalco, A theory for estimation of surface and interfacial energies. III. Estimation of surface energies of solid from contact angle data, J. Phys. Chem. 64 (1960) 561–565.
[32] A.W. Neumann, R.J. Good, C.J. Hope, M. Sejpal, An equation-of-state approach to determine surface tensions of low-energy solids from contact angles, J. Colloid Interface Sci. 49 (1974) 291–304, http://dx.doi.org/10.1016/0021-9797(74)90365-8.
[33] R.J. Good, L. a Girifalco, A theory for estimation of surface and interfacial energies. I. Derivation and application to interfacial tension, J. Phys. Chem. 24 (1960) 561–565, http://dx.doi.org/10.1021/j150553a013.
[34] C.S. Dutcher, A.S. Wexler, S.L. Clegg, Surface tensions of inorganic multicomponent aqueous electrolyte solutions and melts, J. Phys. Chem. A 114 (2010) 12216–12230, http://dx.doi.org/10.1021/jp105191z.
[35] Y. Marcus, Ion Properties, 1997.
[36] Y.S. Kim, L. Dong, A.H. Michael, E.G. Thomas, V. Webb, J.E. McGrath, State of water in disulfonated poly(arylene ether sulfone) copolymers and a perfluorosulfonic acid copolymer (Nafion) and its effect on physical and electrochemical properties, Macromolecules 36 (2003) 17–21.
[37] M.R. Landry, Thermoporometry by differential scanning calorimetry: experimental considerations and applications, Thermochim. Acta 433 (2005) 27–50, http://dx.doi.org/10.1016/j.tca.2005.02.015.
[38] J.B.W. Webber, Studies of nano-structured liquids in confined geometries and at surfaces, Prog. Nucl. Magn. Reson. Spectrosc. 56 (2010) 78–93, http://dx.doi.org/10.1016/j.pnmrs.2009.09.001.
[39] Torben Smith Sorenson, Surface Chemistry and Electrochemistry of Membranes, 1st ed., CRC Press, New York, 1999.
[40] S. Escribano, P. Aldebert, M. Pineri, Volumic electrodes of fuel cells with polymer electrolyte membranes: electrochemical performances and structural analysis by thermoporometry, Electrochim. Acta 43 (1998) 2195–2202.